SP-730
September 2015

Proceedings 22nd ESA Symposium on

European Rocket and Balloon Programmes and Related Research

7–12 June 2015
Tromsø, Norway

Organised by
European Space Agency (ESA)
Andøya Space Center
Centre National d'Études Spatiales (CNES)
Deutschen Zentrums für Luft- und Raumfahrt (DLR)
Swedish Space Corporation (SSC)
Swedish National Space Board (SNSB)
Hochschule Luzern

European Space Agency
Agence spatiale européenne

MEDUSA- MEASUREMENTS OF THE D-REGION PLASMA USING ACTIVE FALLING PLASMA PROBES ON BOARD OF THE REXUS 15 SOUNDING ROCKET

H. Asmus[1], C. Baumann[2], T. Staszak[3], N. Karow[3], P. Schünemann[3], R. E. Mainz[4], A. Fencik[3], E. Jeglorz[1] and B. Strelnikov[1]

[1]*Leibniz Institute of Atmospheric Physics, Schlossstraße 6, 18225 Kühlungsborn, Germany, Email: asmus@iap-kborn.de*
[2]*Deutsches Zentrum für Luft- und Raumfahrt, Institut für Physik der Atmosphäre, Oberpfaffenhofen, Germany , Email: carsten.baumann@dlr.de*
[3]*University of Rostock, Faculty of Mechanical Engineering and Marine Technology, Albert-Einstein-Straße 2, 18059 Rostock, Germany, Email: tristan.staszak@uni-rostock.de*
[4]*Center for Free-Electron Laser Science, c/o DESY, Bldg. 99, Luruper Chaussee 149, 22761 Hamburg, Germany, Email: roland.mainz@cfel.de*

ABSTRACT

A rocket borne experiment was designed to measure the ion density and its relative fluctuations in the lower D-region of the Earth's ionosphere. It was launched on the 29th of May in 2014 at 12 LT during the REXUS 15/16 (Rocket Experiments for University Students) sounding rocket campaign aboard of the REXUS 15 sounding rocket from ESRANGE, Kiruna in northern Sweden. This experiment included two identical FFU's (free falling units) which were ejected on the upper upleg part of the rocket flight and conducted the measurement independently. One of the two FFUs was successfully recovered. It was shown that the developed deployment technique and the FFU framework made by a selective laser sintering process are very suitable for sounding rocket flights and could be the carrier system for any kind of small scientific instrument. The results of the measurement of the fixed-biased probe showed reasonable ion densities for the up- and downleg phase of the FFU flight. A spectral analysis of the data showed no significant turbulence.

Key words: D-region, ionosphere plasma, in situ technique.

1. INTRODUCTION

The polar D-region recently got into the focus of atmospheric research being the host of numerous phenomena linked to dusty plasma irregularities and neutral turbulence. These phenomena are e.g., polar mesospheric winter echoes (PMWE) observed by radar in an altitude range between 55 and 85 km [3, 5, 8, 9] which could be useful to study atmospheric parameters like winds or turbulence. In order to obtain these parameters it is necessary to understand the underlying physics of the phenomena itself. The physical processes of PMWE are still not fully understood and are under ongoing investigation in the middle Atmosphere science community. To investigate the creation process of PMWE caused refractive index fluctuations at the radar bragg scale (e.g. 3 m for 50 MHz radar) it is important to get information of the horizontal variance and vertical fine structure of the lower D-region plasma. Since the ion density irregularities at these heights are strongly coupled to the neutral turbulence, one can use ion density fluctuations as a tracer of turbulent motions [2, 1]. This paper presents a student experiment measuring relative ion densities with free falling units. Sec. 2 will briefly introduce the principle used to measure relative ion density. Sec. 3 will then give an overview about the technical aspects of the experiment divided into on board systems and FFU design. The experiments results are presented in Sec. 4 and are summarized in Sec. 5.

2. EXPERIMENT PRINCIPLE

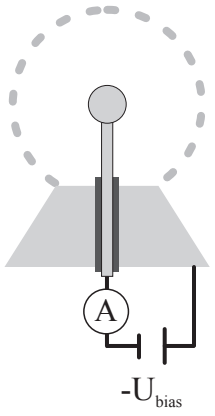

Figure 1: Principle sketch of the fixed-biased probe.

The experiment principle follows the ideas from [10, 6, 2, 1] where a fixed-biased langmuir probe is used to obtain relative positive ion densities. Fig. 1 shows a principle sketch of the used probe. The spherical probe is centered in a gridded sphere which is at payload or floating potential whereas the probe in the center is biased negatively with respect to the payload. The probe therefore attracts positive ions and repels electrons. The measured current between the negative probe and the FFU framework is propor-

Proc. '22nd ESA Symposium on European Rocket and Balloon Programmes and Related Research', Tromsø, Norway, 7–12 June 2015 (ESA SP-730, September 2015)

tional to the ion density which can be calculated by using the following equation [10]

$$I_i = \pi r^2 N_i q_e v_{th} f(V) \left[\frac{1}{2} e^{-x^2} + \sqrt{\pi} \left(\frac{x}{2} + \frac{1}{4x} \right) \mathrm{erf}(x) \right], \quad (1)$$

where I_i is the measured current, $x = 2v_r/\sqrt{\pi}v_{th}$, v_r is the FFU velocity, r is the radius of the spherical grid, N_i is the ion density, q_e is the elementary charge, v_{th} is the ion thermal velocity and finally $f(V)$ is a function of the payload potential which is set to unity assuming negligible changes of the potential during the flight.

The obtained ion density is a relative density and hence has to be normalized to an absolute density at a reasonable altitude.

3. ENGINEERING

The MEDUSA experiment consisted of two free flying units (FFUs) which were mounted inside the main payload by an ejection mechanism. The experiment can therefor be divided into two parts. Firstly, the Systems on board the main payload and secondly, the FFU design itself. These parts will be described in the following subsections, each subdivided into a mechanical and an electronical part.

3.1. Systems on board the main payload

The FFU Ejection System was the mechanical subsystem on board the main payload. It carried the FFUs inside the rocket and caused the ejection of the FFUs. The electronical subsystem is called On board Control Unit (OCU) and provides the electrical interface between the experiment and the REXUS service module (RXSM). All parts on board the main payload were mounted on a bulkhead in a standard 14" 300 mm module.

3.1.1. FFU Ejection System

The FFUs were ejected through orifices in the module wall. These were closed by ejectable hatches until the ejection of the FFUs. Therefore they were hold in place by steel wires and loaded by springs. To open the hatches the wires were cut by a pyrocutter. One hatch system is shown as a CAD drawing in Fig. 2. Two seconds after the hatch opening the FFUs were ejected. The ejection mechanism was mainly based on the rifled barrel principle, which demanded an ejection barrel for each FFU. The FFUs were hold inside the ejection barrels by spring loaded stamps, which can be seen red in Fig. 3. Until ejection a steel wire held down these stamps. The wires were cut by pyrocutters and the fixation stamps released

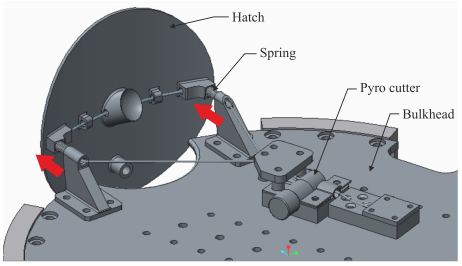

Figure 2: CAD drawing of one hatch system including fixation wires, ejection springs and pyrocutter.

the FFUs. During ejection a spring in the end of the ejection barrel accelerate the FFUs with a maximum force of 229 N. The ejection barrels were tilted by 30° relative to the x-y plane of the rocket to ensure that the initial pointing direction of the FFU front was likely towards the Earth's surface. The side view of the ejection mechanism

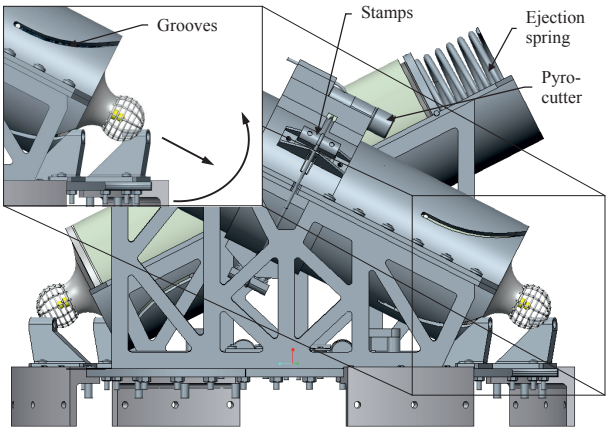

Figure 3: Rifled barrel principle. See description in the text.

in Fig. 3 demonstrates the riffled barrel principle. Guiding pins on the FFU framework are lead by the helical grooves of the ejection barrel. The grooves are curved in a way, that for the given acceleration of the springs, the FFU reach a spin rate of 8 Hz after leaving the ejection barrel. This guaranteed a stable flight during the FFU's free fall phase.

3.1.2. OCU- On board Control Unit

The OCU was placed below the ejection mechanism on the bottom side of the bulkhead where it was connected to the RXSM and the FFUs. It delivers communication inter structure between FFUs and RXSM and also ensured the charging of the FFUs. The OCU was also able to receive the signals liftoff (LO), start of experiment (SOE) and start of data storage (SODS) from the RXSM.

3.2. FFU design

The FFU's design was chosen to be cylindrical because of hatch size limitations. The fixed-biased langmuir probe was placed on one end of the cylinder which was meant to be in flight direction during downleg. Parachute and recovery systems were placed on the opposite side.

3.2.1. Mechanics

The FFU's framework was made of Al_6Ti_4V alloy in a selective laser sintering process which allowed high robustness for thin structures. This technique allowed us to maximize the available space ,which was needed for the electronics, the batteries and the parachute system. The

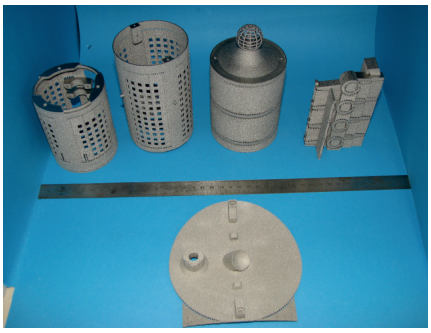

Figure 4: FFU framework and hatch made in a selective sintering process. The steel scale on the picture is 30 cm long.

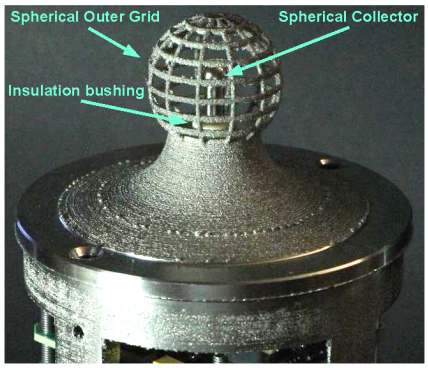

Figure 5: FFU nose cone with the positive ion probe.

FFU's hull was made of Polytetrafluoroethylene (PTFE) which is insulating and has a very low coefficient of friction against solids. These properties became important in terms of minimizing friction during the ejection and receiving GPS signals inside the FFUs. Fig. 4 shows all the parts made by the selective sintering process shortly after manufacturing which are the FFU cone with the grid, the FFU framework and the hatches for the rocket module. These parts were post processed to satisfy the experiment requirements in terms of mechanical accuracy. An annotated view of the nose cone of the FFU with the positive ion probe can bee seen in Fig. 5. Fig. 6 and 7 show CAD drawings of the FFU back with the back cover opening system.

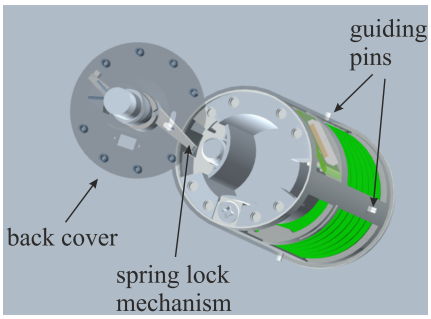

Figure 6: FFU frame work and back cover from the back side view.

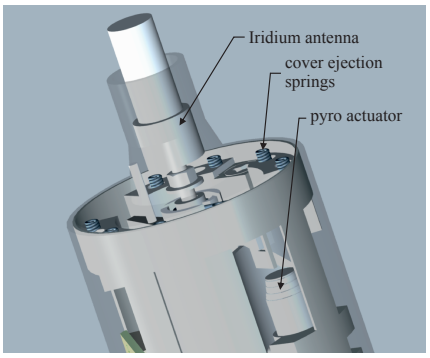

Figure 7: Side view of the rear with the back cover.

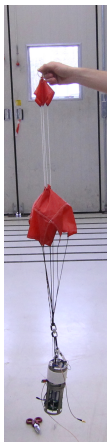

Figure 8: Parachute System.

The parachute system consisted of a pilot and a main chute (see Fig. 8). This system included the beacon antenna which was wrapped around one parachute fixation rope and was packed into a 3d-printed plastic container made of ABS (Acrylonitrile butadiene styrene) in the rear of the FFU. The ejection was performed by a spring lock mechanism (Fig. 6 & 7) which was opened by a pyro actuator. Therefore the lock had one sloping surface which was used to open the lock when the pin of the pyro actuator pressed onto it. After the lock was open, the back cover was then pushed out by springs (see Fig. 7) and additionally pulled out the pilot chute. This opening event was triggered by an pressure sensor giving a dedicated signal at 5 km as well as an predefined time line event as back up.

3.2.2. Electronics

To measure the current between the negative biased probe and the FFU's framework a current-to-voltage converting amplifier was used. An analog-to-digital converter with a sampling rate of 10 kSa/s was chosen for the sensor current to verify a high spatial resolution ($\sim$cm). Since the

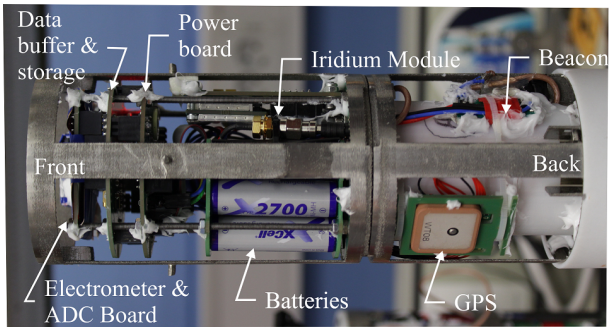

Figure 9: Side view of FFU without PTFE hull with the placement of the electronics.

FFUs should been recovered the electronics on board of the FFUs included besides the sensor electronics, a commercial GPS module, an Iridium satellite module and a radio beacon. As mentioned in seq. 3.1 the recovery subsystems were activated by a pressure sensor and a time line event. The measured sensor current and the housekeeping data were stored on a SD-card. Fig. 9 shows the arrangement of the electronics. The circuit boards and the battery pack could be stacked together and were mounted onto threaded rods.

4. RESULTS

The following section presents a short summary of the experiments performance, failure analysis and the obtained scientific results.

4.1. Performance

The criteria for a successful flight was the recovery and extracting the data of at least one FFU. According to this criteria we are fully satisfied with the obtained results. Fig. 10 shows the trajectory of the REXUS 15 main payload obtained from GPS data. The red dots indicated positions of the FFUs during ejection as well as the main payloads and the recovery position of one FFU. This FFU (1) was found 4.3 km southwestern of the main payload and about 40 km northwestern from the ESRANGE.

The following list shows the critical elements and its performance ($\surd$ - full, ($\surd$)- partly, $\times$ - fail, ? - unknown):

Element		FFU 1	FFU 2
Hatch Ejection		$\surd$	($\surd$)
FFU Ejection		$\surd$	$\surd$
Recovery system	Parachute	($\surd$)	?
	Beacon	($\surd$)	$\times$
	GPS	$\times$	$\times$
	Iridium	$\surd$	$\surd$
SD Card		$\surd$	?

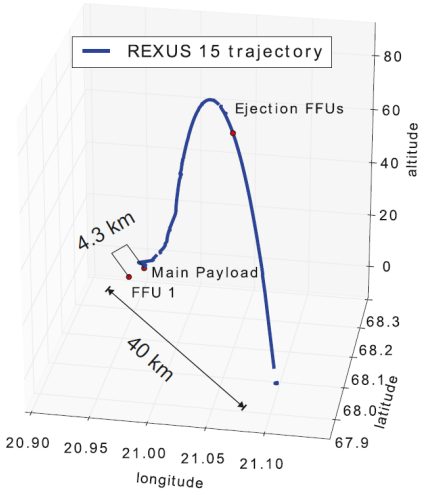

Figure 10: Trajectory of the main payload and the position of the recovered FFU 1.

The performance of the hatch ejection and the ejection of the FFUs has been validated via two side looking cameras inside the StrathSat module which was located below the MEDUSA module [4]. The performance of the parachute system which could be analyzed was found to be a partly success. The main chute was still folded since one of the pilot chute rope was wrapped around the back cover and hence the pilot chute was not able to pull out the main chute.

In total there were three messages from the Iridium module which should have send the GPS coordinates, but the GPS itself did not give a position. We used the rough position of the Iridium module which was also included in the message. Further error analysis can be found in Sec. 4.2.

Using wavelet analysis of the measured ion current we found a clear spin modulation during up- and downleg which corresponds to a spin frequency of around 8 Hz. This also could be reproduced from the StrathSat video material giving $\sim$7.5 Hz spin rate. We take this as a proof for the successful spin stabilization of the recovered FFU.

4.2. Failure analysis

The analysis of the StrathSat video material also gave rise to the conclusion that one of the hatches did not fully eject. This was found to be the hatch of the lost FFU. Although a connection between both circumstances could not be proven. One main issue was the timing of the pyro actuator which included the ejection of the parachute as well as the activation of the GPS, the Iridium module and the beacon. The backup system for the activation of the FFU recovery system was based on a simple simulation of the FFUs free fall. The time of the ejection was actually set too early. The parachute ejection and the recovery system power-on occurred already at an altitude of $\sim$20 instead of planned 5 km. This probably activated a whole

chain of malfunctions. The insufficient unfolding of the parachute due to less aerodynamical friction, the unfavorable unfolding of the beacon antenna, the GPS malfunction because of the wrong altitude and an too early shut down of the system. The shut down was planned and realizised to be 3 h after parachute ejection, but the recovery crew started looking for the FFUs only after 2.5h. Therefore they found the first FFU, but could not found the second one, as it already stopped transmitting a beacon signal.

4.3. Scientific results

From the measured currents of the recovered FFU the relative ion density could be calculated using Eq. 1. The temperature was taken from MSIS model data [7]. The FFU velocity was assumed to be the same as the main payloads velocity neglecting the ejecting speed of around 1.8 ms^{-1}. The relative density was then normalized to the absolute electron density obtained by the EISCAT radar at 80 km assuming that electron and ion densities are equal at these heights. Fig. 11 shows the smoothed profiles of the ion density for upleg (red) and for downleg (black). The grey line shows the full reso-

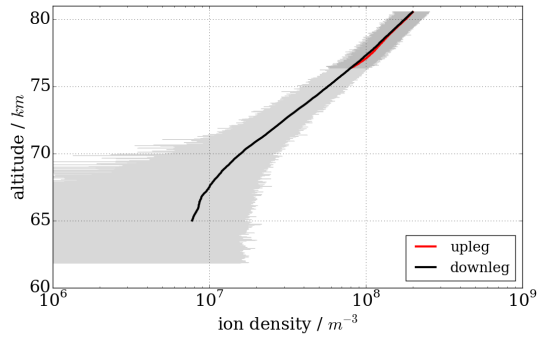

Figure 11: Ion density normalized to the absolute electron density at 80 km obtained by the EISCAT radar.

lution data. Having a Kp index around 2 for the launch day the ionospheric conditions were quiet. This also can be confirmed by the ESRAD radar observations (Fig. 12) which showed no signals during the rocket flight. Besides, shortly after the rocket launch a PMSE occurred between 80 and 90 km which indicates the presence of charged ice particles and nevertheless this does not have an impact on the presented results.

The derived absolute values of the ion density are reasonable for quiet ionospheric conditions. During the upleg part of the flight the sensor was in an unfavorable position being in the wake. On the downleg phase there seems to be no fine structure at all. If one calculates the residuals of the ion density $\Delta n_i = \frac{N_i - \langle N_i \rangle}{\langle N_i \rangle}$ and do the wavelet transform, one receives the wavelet power spectra which can be seen in Fig. 13. The wavelet spectra show no

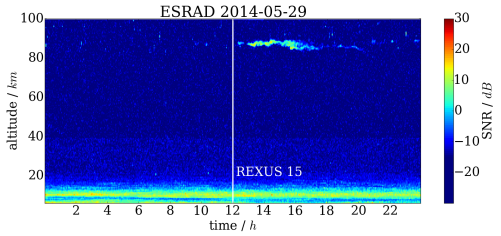

Figure 12: ESRAD SNR for the launch day. PMSE occured shortly after launch.

significant structures on the downleg phase. We therefor conclude that there were no observable plasma irregularities or neutral turbulence during that flight. In addition one can see that the noise level (green) is relatively high as also mentioned in Sec. 4.2.

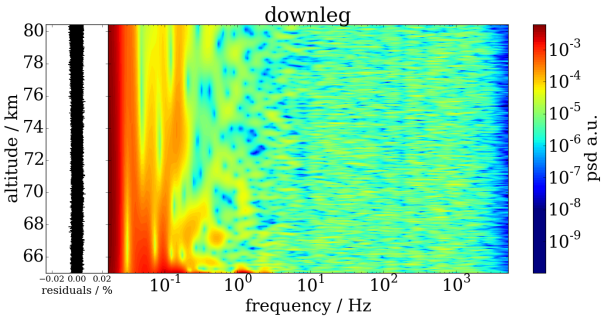

Figure 13: Wavelet power spectra of the ion density residuals after filtering the spin modulation

5. CONCLUSIONS

A new ejection system for cylindrical free falling units was developed and successfully tested on board of a sounding rocket. Also the fairly new techniques of selective laser sintering and 3D-printing were successfully used in a sounding rocket experiment. Several subsystems of the experiment e.g. ejection system and FFUs can be improved in terms of susceptibility to malfunctions and sensitivity. Besides the technical success, a quiet lower D-region was probed in-situ and a ion density profile could be obtained which is comparable to other measurements with similar ionospheric conditions. The developed ejection mechanism is suitable for any kind of scientific instrument and can be used in future projects.

ACKNOWLEDGMENTS

We are grateful for the help and the support from our home institutes (IAP, University of Rostock and IPA) as well as DLR and ZARM. We also appreciate the provision of data to compare our measurement with. Here we

would like to thank Irina Strelnikova, Sheila Kirkwood and the StrathSat Team.

REFERENCES

[1] A. Brattli, T. A. Blix, Ø. Lie-Svendsen, U.-P. Hoppe, F.-J. Lübken, M. Rapp, W. Singer, R. Latteck, and M. Friedrich. Rocket measurements of positive ions during polar mesosphere winter echo conditions. *Atmospheric Chemistry and Physics*, 6(12):5515–5524, 2006.

[2] T. A. Blix, E. V. Thrane, and Ø. Andreassen. In situ measurements of the fine-scale structure and turbulence in the mesosphere and lower thermosphere by means of electrostatic positive ion probes. *Journal of Geophysical Research*, 95(D5):5533, 1990.

[3] P. Czechowsky, R. Rüster, and G. Schmidt. Variations of mesospheric structures in different seasons. *Geophysical Research Letters*, 6(6):459–462, 1979.

[4] N. L. Donaldson, R. A. Clark, T. Sinn, D. Garcia-Yarnoz, C. Lowe, T. Parry, P. Hammond, R. Brown StrathSat-R2: Deployable Structure Demonstrator on REXUS 15. *Proceedings of the 22th ESA Symposium on European Rocket and Balloon Programmes and Related Research*, 7-12 June 2015, Tromsø, Norway

[5] W. L. Ecklund and B. B. Balsley. Long-term observations of the arctic mesosphere with the MST radar at Poker Flat, Alaska. *Journal of Geophysical Research*, 86(A9):7775, 1981.

[6] K. Folkestad. *Ionospheric Studies by in situ Measurements in Sounding Rockets*. PhD thesis, University of Oslo, Oslo, 1970.

[7] A. E. Hedin. Extension of the MSIS thermosphere model into the middle and lower atmosphere. *Journal of Geophysical Research*, 96(A2):1159, 1991.

[8] S. Kirkwood, V. Barabash, E. Belova, H. Nilsson, T. N. Rao, K. Stebel, A. Osepian, and P. B. Chilson. Polar mesosphere winter echoes during solar proton events. *Adv. polar Upper Atmos. Res.*, (16), 2002.

[9] F.-J. Lübken, B. Strelnikov, M. Rapp, W. Singer, R. Latteck, A. Brattli, U.-P. Hoppe, and M. Friedrich. The thermal and dynamical state of the atmosphere during polar mesosphere winter echoes. *Atmospheric Chemistry and Physics*, 6(1):13–24, 2006.

[10] R. C. Sagalyn, M. Smiddy, and J. Wisnia. Measurement and interpretation of ion density distributions in the daytime F region. *Journal of Geophysical Research*, 68(1):199–211, 1963.